PROCEEDINGS OF SCIENCE

Confronting next-to-leading order CGC/Saturation approach with HERA data

José Garrido,[a,*] **Miguel Guevara**[b] **and Michael Sanhueza**[b,c]

[a] *Departamento de Física, Universidad Técnica Federico Santa María, Avda. España 1680, Casilla 110-V, Valparaíso, Chile*

[b] *Facultad de Ingeniería, Laboratorio DataScience, Universidad de Playa Ancha, Leopoldo Carvallo 270, Valparaíso, Chile*

[c] *Centro de Estudios Avanzados, Universidad de Playa Ancha, Traslaviña 450, Viña del Mar, Chile*

E-mail: jose.garridom@sansano.usm.cl, miguel.guevara@upla.cl, michael.roa@upla.cl

In this talk, we present an analysis of the next-to-leading order CGC/saturation approach from Ref. [1] using combined HERA data to determine its parameters. The model features an analytical solution for the non-linear Balitsky-Kovchegov (BK) evolution equation and an exponential behavior of the saturation momentum with impact parameter b-dependence, characterized by $Q_s \propto \exp(-mb)$. With its parameters fixed via a fit to high-precision HERA data, we compare the model predictions with experimental data at small-x for the proton structure function F_2, longitudinal structure function F_L and exclusive vector meson production. The model shows excellent agreement across a wide kinematic range of Q^2 at small-x, supporting its use for reliable predictions in upcoming experiments like the Electron-Ion Collider and the LHeC.

31st International Workshop on Deep Inelastic Scattering (DIS2024)
8–12 April 2024
Grenoble, France

*Speaker

PoS(DIS2024)092

1. Introduction

The Color Glass Condensate (CGC)/saturation effective field theory [2] provides an effective description of high-energy QCD processes. However, leading-order CGC predictions show high-energy growth inconsistent with experimental data. To address this, in Ref. [1] non-linear corrections were introduced to the BFKL kernel [3] of the Balitsky-Kovchegov (BK) equation [4], complemented by a resummation procedure [5] that accurately solves this problem. Additionally, this approach incorporates a saturation momentum formulation designed to satisfy the Froissart theorem [6] and ensure consistency in the large impact parameter (b) limit. Applying this enhanced CGC/saturation dipole model to precise HERA DIS data [7, 8], we extracted phenomenological parameters and confronted theoretical predictions with experimental results for various observables.

2. Inclusive and Exclusive Processes

The proton structure functions can be expressed in terms of the virtual photon-proton cross section $\sigma^{\gamma^* p}$ as follows:

$$F_2\left(Q^2, x\right) = \frac{Q^2}{4\,\pi^2\,\alpha_{\rm e.m.}} \left[\sigma_T^{\gamma^* p}(Q^2, x) + \sigma_L^{\gamma^* p}(Q^2, x)\right], \tag{2.1}$$

$$F_L\left(Q^2, x\right) = \frac{Q^2}{4\,\pi^2\,\alpha_{\rm e.m.}}\, \sigma_L^{\gamma^* p}(Q^2, x), \tag{2.2}$$

where the virtual photon-proton cross section can be calculated in the CGC framework as

$$\sigma_{T,L}^{\gamma^* p}(Q^2, x) = 2 \int d^2 b \int \frac{d^2 r}{4\pi} \int_0^1 dz\, |\Psi_{L,T}^{\gamma^*}(Q, r, z)|^2\, N(r, Y; b)\,, \tag{2.3}$$

with $Y = \ln(1/x_{Bj})$, x_{Bj} is the Bjorken x, z is the fraction of the virtual photon momentum carried by the quark, and Q is the photon virtuality. The $|\Psi_{L,T}^{\gamma^*}(Q, r, z)|^2$ are the overlap wave-functions of the photon, detailed in Ref. [2], and $N(r, Y; b)$ represents the imaginary part of the forward $q\bar{q}$ dipole-proton scattering amplitude with transverse dipole size r and impact parameter b. For exclusive diffractive processes $\gamma^* + p \longrightarrow E + p$ (where E is a real photon in DVCS or a vector meson), the amplitude and differential cross-section are given by:

$$\mathcal{A}_{T,L}^{\gamma^* p \to E p}(x, Q, \Delta) = 2i \int d^2\boldsymbol{r} \int_0^1 \frac{dz}{4\pi} \int d^2\boldsymbol{b}\, (\Psi_E^* \Psi)_{T,L}\, \mathrm{e}^{-i[\boldsymbol{b} - (\frac{1}{2} - z)\boldsymbol{r}]\cdot\boldsymbol{\Delta}}\, N(r, Y; b)\,, \tag{2.4}$$

$$\frac{d\sigma_{T,L}^{\gamma^* p \to E p}}{dt} = \frac{1}{16\pi} \left|\mathcal{A}_{T,L}^{\gamma^* p \to E p}\right|^2 (1 + \beta^2), \tag{2.5}$$

where the expressions for the overlap wave functions can be found in Ref. [9] and β accounts for the ratio of the real to imaginary parts of the scattering amplitude. Two main observables used in the analysis are the total cross-section $\sigma_{T,L}^{\gamma^* p \to E p}$ and the slope parameter B_D, defined as:

$$\sigma_{T,L}^{\gamma^* p \to E p} = \int dt \frac{d\sigma_{T,L}^{\gamma^* p \to E p}}{dt} \quad , \quad B_D = \lim_{t \to 0} \frac{d}{dt} \ln\left(\frac{d\sigma_{T,L}^{\gamma^* p \to E p}}{dt}\right). \tag{2.6}$$

3. CGC/saturation dipole model

The color $q\bar{q}$ dipole-proton scattering amplitude $N(r, Y; b)$ in the model of [1] is given by:

$$N(z) = \begin{cases} N_0\, e^{z\bar{\gamma}} & \text{for } \tau \le 1, \\ a\left(1 - e^{-\Omega(z)}\right) + (1-a)\,\frac{\Omega(z)}{1+\Omega(z)} & \text{for } \tau > 1, \end{cases} \tag{3.1}$$

where $a = 0.65$, $z = \ln\left(r^2 Q_s^2(Y, b)\right)$ and $\Omega(z)$ is:

$$\Omega(z) = \Omega_0 \left\{ \cosh\left(\sqrt{\sigma} z\right) + \frac{\bar{\gamma}}{\sqrt{\sigma}} \sinh\left(\sqrt{\sigma} z\right) \right\}, \quad \sigma = \frac{\bar{\alpha}_S}{\lambda(1+\bar{\alpha}_S)}. \tag{3.2}$$

We use the following expression to represent the saturation momentum:

$$Q_s^2(Y, b) = Q_0^2 (m\, b\, K_1(m\, b))^{1/\bar{\gamma}} e^{\lambda Y}, \tag{3.3}$$

where the critical anomalous dimension $\bar{\gamma}$ and energy behavior of the saturation scale λ are:

$$\bar{\gamma} = \bar{\gamma}_\eta (1 + \lambda_\eta), \qquad \bar{\gamma}_\eta = \sqrt{2 + \bar{\alpha}_S} - 1, \tag{3.4}$$

$$\lambda = \frac{\lambda_\eta}{1 + \lambda_\eta}, \quad \lambda_\eta = \frac{1}{2} \frac{\bar{\alpha}_S}{3 + \bar{\alpha}_S - 2\sqrt{2 + \bar{\alpha}_S}}. \tag{3.5}$$

Expanding the linear solution of Eq. (3.1) to $\tau < 1$, we replace $\bar{\gamma}$ by:

$$\bar{\gamma} \to \bar{\gamma} + \frac{\ln(1/\tau)}{2\kappa\lambda Y}, \quad \kappa = \frac{\chi''(\bar{\gamma})}{\chi'(\bar{\gamma})} = \frac{\frac{d^2\omega(\bar{\gamma}_\eta)}{d\bar{\gamma}_\eta^2}}{\frac{d\omega(\bar{\gamma}_\eta)}{d\bar{\gamma}_\eta}}. \tag{3.6}$$

This equation was derived in Ref. [10] and has demonstrated a strong agreement with the experimental data for $x \le 0.01$.

4. Numerical results and discussion

The model uses four parameters fitted to H1 and ZEUS data [7], and the fit range $0.85\,\text{GeV}^2 < \text{Q}^2 < 30\,\text{GeV}^2$ and $x \le 10^{-2}$ ensures BK equation validity, with χ^2 minimization including systematic and statistical uncertainties.

Dipole amplitude				Minimization
$\bar{\alpha}_S$	N_0	Q_0^2 (GeV^2)	m (GeV)	χ^2/d.o.f.
0.1040 $\pm 4.6 \times 10^{-4}$	0.1311 $\pm 3.7 \times 10^{-4}$	0.797 $\pm 3.3 \times 10^{-3}$	0.4743 $\pm 9.6 \times 10^{-4}$	205.70/166 = 1.239
0.1100 $\pm 1.8 \times 10^{-4}$	0.1510 $\pm 8.1 \times 10^{-4}$	0.809 $\pm 6.2 \times 10^{-3}$	0.5412 $\pm 1.8 \times 10^{-4}$	204.73/166 = 1.233

Table 1: Parameters of the CGC/saturation dipole model for fixed light quark masses $10^{-2} \div 10^{-4}$ and two fixed values of the charm quark masses, 1.40 GeV (first line) and 1.27 GeV (second line) respectively.

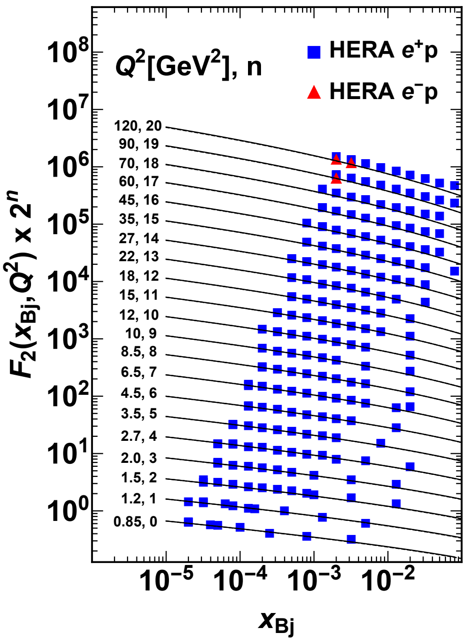

Fig. 1-a

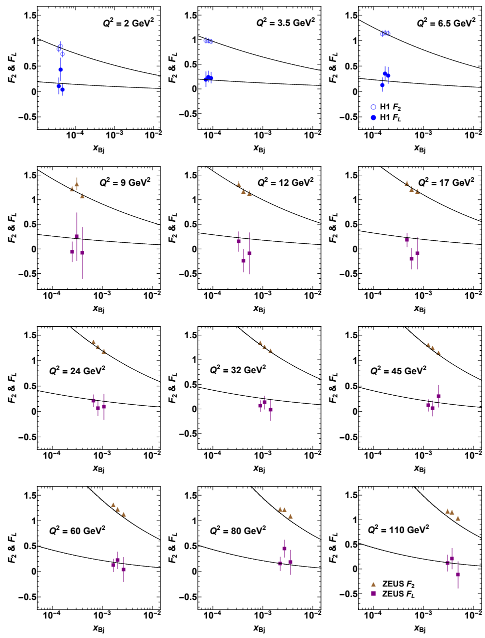

Fig. 1-b

Figure 1: Fig. 1-a: Structure function $F_2(x,Q^2)$ vs x, for different Q^2 values. Theoretical results and experimental data from H1 and ZEUS [7]. Fig. 1-b: Results for the longitudinal structure function $F_L(x,Q^2)$ and the structure function $F_2(x,Q^2)$, as functions of x, for different values of Q^2. The solid and dashed lines are generated using parameter sets from table I, which correspond to charm masses of $m_c = 1.4\,\text{GeV}$ and $m_c = 1.27\,\text{GeV}$, respectively. The experimental data are from ZEUS and H1 collaboration [11, 12].

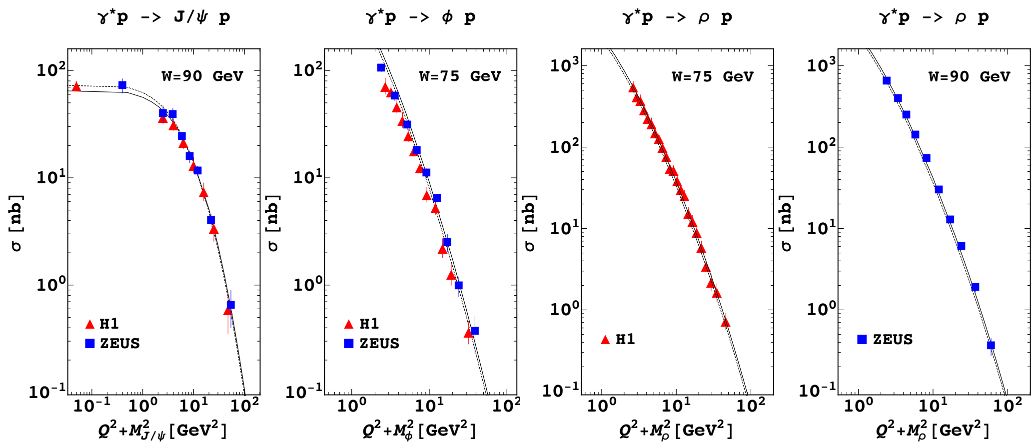

Figure 2: Total vector meson cross-sections σ for J/ψ, ϕ and ρ, as a function of $Q^2 + M_E^2$ compared to theoretical estimates from CGC/saturation dipole model where solid ($m_c = 1.4\,\text{GeV}$) and dashed ($m_c = 1.27\,\text{GeV}$) lines correspond to the parameters used from table I, respectively. The data are from H1 and ZEUS collaborations [13–18].

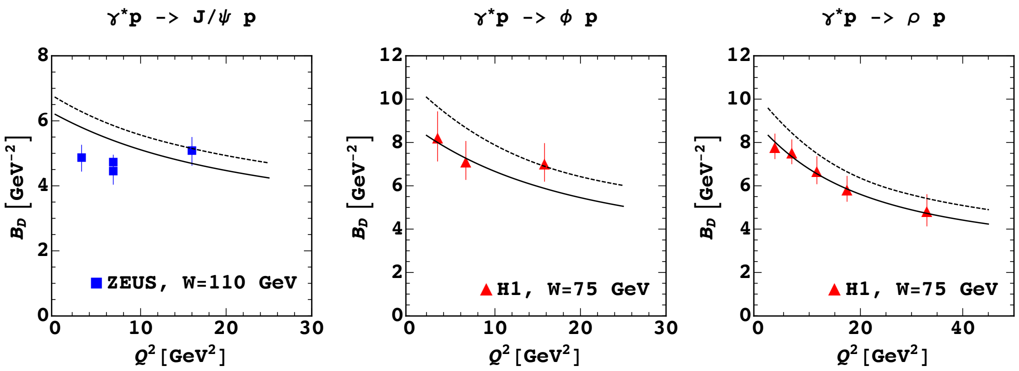

Figure 3: Results for the slope B_D of $t-$distribution of exclusive vector meson electroproduction as a function of Q^2. Solid and dashed lines represent calculations using charm quark masses of m_c = 1.4 GeV and m_c = 1.27 GeV, respectively, from table I. The collection of experimental data are from H1 and ZEUS collaborations [13–18].

The results show that with only four parameters fixed by the reduced cross-section, this model provides a good description of nearly all available data on inclusive and exclusive diffractive processes at HERA for small-x ($x \leq 10^{-2}$). For a comparison of our results with other observables at HERA, refer to Ref. [19].

5. Acknowledgements

This work was supported by Grant PIIC No. 008/2023 and by PhD scholarship No. 029/2023, from DPP, USM (JG), and by Plan de Fortalecimiento de Universidades Estatales, UPA 19101, CR 18.180, Código 2390, Universidad de Playa Ancha and ANID Grant No 3230699 (MS). J.G. also thanks to Fondecyt (Chile) grant 1231829 and InES I+D Institutional project, code INID210013/INID202303 of UPLA for financial support to attend the DIS2024 workshop.

References

[1] C. Contreras, E. Levin, R. Meneses and M. Sanhueza, *"Non-linear equation in the re-summed next-to-leading order of perturbative QCD: the leading twist approximation,"* Eur. Phys. J. C **80** (2020) no.11, 1029 [arXiv:2007.06214 [hep-ph]].

[2] Yuri V Kovchegov and Eugene Levin, *"Quantum Choromodynamics at High Energies"*, Cambridge Monographs on Particle Physics, Nuclear Physics and Cosmology, Cambridge University Press, 2012 .

[3] V. S. Fadin, E. A. Kuraev and L. N. Lipatov, *"On the pomeranchuk singularity in asymptotically free theories"*, Phys. Lett. **B60**, 50 (1975); E. A. Kuraev, L. N. Lipatov and V. S. Fadin, *"The Pomeranchuk Singularity in Nonabelian Gauge Theories"* Sov. Phys. JETP **45**, 199 (1977), [Zh. Eksp. Teor. Fiz.72,377(1977)]; I. I. Balitsky and L. N. Lipatov, *"The Pomeranchuk Singularity in Quantum Chromodynamics,"* Sov. J. Nucl. Phys. **28**, 822 (1978), [Yad. Fiz.28,1597(1978)].

[4] I. Balitsky, [arXiv:hep-ph/9509348]; Phys. Rev. **D60**, 014020 (1999) [arXiv:hep-ph/9812311]; Y. V. Kovchegov, Phys. Rev. **D60**, 034008 (1999), [arXiv:hep-ph/9901281].

[5] G. P. Salam, *"A Resummation of large subleading corrections at small x,"* JHEP **9807** (1998) 019 [hep-ph/9806482];

[6] M. Froissart, *Phys. Rev.* **123** (1961) 1053;
A. Martin, "Scattering Theory: Unitarity, Analitysity and Crossing." Lecture Notes in Physics, Springer-Verlag, Berlin-Heidelberg-New-York, 1969.

[7] F. D. Aaron *et al.* [H1 and ZEUS Collaborations], *"Combined Measurement and QCD Analysis of the Inclusive ep Scattering Cross Sections at HERA,"* JHEP **1001** (2010) 109 [arXiv:0911.0884 [hep-ex]].

[8] H. Abramowicz *et al.* [H1 and ZEUS Collaborations], *"Combination and QCD Analysis of Charm Production Cross Section Measurements in Deep-Inelastic ep Scattering at HERA,"* Eur. Phys. J. C **73** (2013) 2, 2311 [arXiv:1211.1182 [hep-ex]].

[9] H. Kowalski, L. Motyka and G. Watt, *"Exclusive diffractive processes at HERA within the dipole picture,"* Phys. Rev. **D74** (2006) 074016 [hep-ph/0606272].

[10] E. Iancu, K. Itakura and L. McLerran, *"Geometric scaling above the saturation scale,"* Nucl. Phys. **A708** (2002) 327 [hep-ph/0203137].

[11] H. Abramowicz *et al.* [ZEUS Collaboration], *"Deep inelastic cross-section measurements at large y with the ZEUS detector at HERA,"* Phys. Rev. **D90** (2014) 7, 072002 [arXiv:1404.6376 [hep-ex]]; S. Chekanov *et al.* [ZEUS Collaboration], *"Measurement of the Longitudinal Proton Structure Function at HERA,"* Phys. Lett. **B682** (2009) 8 [arXiv:0904.1092 [hep-ex]].

[12] V. Andreev *et al.* [H1], "Measurement of inclusive ep cross sections at high Q^2 at $\sqrt{s} = 225$ and 252 GeV and of the longitudinal proton structure function F_L at HERA," Eur. Phys. J. C **74**, no.4, 2814 (2014) [arXiv:1312.4821 [hep-ex]].

[13] S. Chekanov *et al.* [ZEUS], PMC Phys. A **1**, 6 (2007) [arXiv:0708.1478 [hep-ex]].

[14] S. Chekanov *et al.* [ZEUS], Eur. Phys. J. C **24**, 345-360 (2002) [arXiv:hep-ex/0201043 [hep-ex]].

[15] S. Chekanov *et al.* [ZEUS], Nucl. Phys. B **695**, 3-37 (2004) [arXiv:hep-ex/0404008 [hep-ex]].

[16] A. Aktas *et al.* [H1], Eur. Phys. J. C **46**, 585-603 (2006) [arXiv:hep-ex/0510016 [hep-ex]].

[17] S. Chekanov *et al.* [ZEUS], Nucl. Phys. B **718**, 3-31 (2005) [arXiv:hep-ex/0504010 [hep-ex]].

[18] F. D. Aaron *et al.* [H1], JHEP **05**, 032 (2010) [arXiv:0910.5831 [hep-ex]].

[19] M. Sanhueza, J. Garrido and M. Guevara, "CGC/saturation approach: Impact-parameter dependent model in next-to-leading order of perturbative QCD and combined HERA data," [arXiv:2311.06406 [hep-ph]].